PNAS RESEARCH ARTICLE | IMMUNOLOGY AND INFLAMMATION OPEN ACCESS

Characteristics and anatomic location of PD-1$^+$TCF1$^+$ stem-like CD8 T cells in chronic viral infection and cancer

Se Jin Im[a,b,c,1,2], Rebecca C. Obeng[a,b,d,e,1], Tahseen H. Nasti[a,b], Daniel McManus[a,b], Alice O. Kamphorst[f,g], Sivaram Gunisetty[a,b], Nataliya Prokhnevska[a,h], Jennifer W. Carlisle[i,j], Ke Yu[d], Gabriel L. Sica[d,j,k], Lucas E. Cardozo[l], André N. A. Gonçalves[l], Haydn T. Kissick[a,h], Helder I. Nakaya[l], Suresh S. Ramalingam[i,j,2], and Rafi Ahmed[a,b,2]

Contributed by Rafi Ahmed; received December 29, 2022; accepted August 31, 2023; reviewed by Daniel Chen and Pavan Reddy

CD8 T cells play an essential role in antitumor immunity and chronic viral infections. Recent findings have delineated the differentiation pathway of CD8 T cells in accordance with the progenitor-progeny relationship of TCF1$^+$ stem-like and Tim-3$^+$TCF1$^-$ more differentiated T cells. Here, we investigated the characteristics of stem-like and differentiated CD8 T cells isolated from several murine tumor models and human lung cancer samples in terms of phenotypic and transcriptional features as well as their location compared to virus-specific CD8 T cells in the chronically lymphocytic choriomeningitis virus (LCMV)-infected mice. We found that CD8 tumor-infiltrating lymphocytes (TILs) in both murine and human tumors exhibited overall similar phenotypic and transcriptional characteristics compared to corresponding subsets in the spleen of chronically infected mice. Moreover, stem-like CD8 TILs exclusively responded and produced effector-like progeny CD8 T cells in vivo after antigenic restimulation, confirming their lineage relationship and the proliferative potential of stem-like CD8 TILs. Most importantly, similar to the preferential localization of PD-1$^+$ stem-like CD8 T cells in T cell zones of the spleen during chronic LCMV infection, we found that the PD-1$^+$ stem-like CD8 TILs in lung cancer samples are preferentially located not in the tumor parenchyma but in tertiary lymphoid structures (TLSs). The stem-like CD8 T cells are present in TLSs located within and at the periphery of the tumor, as well as in TLSs closely adjacent to the tumor parenchyma. These findings suggest that TLSs provide a protective niche to support the quiescence and maintenance of stem-like CD8 T cells in the tumor.

stem-like CD8 T cells | chronic viral infection | cancer models | human lung cancer | tertiary lymphoid structures

CD8 T cell immunity is important against chronic viral infections and cancer (1, 2). However, persistent antigenic stimulation leads to the functional impairment of antigen-specific CD8 T cells, also called T cell exhaustion, with high expression of inhibitory receptors, most notably programmed death 1 (PD-1) (1–5). PD-1-targeted immunotherapies are known to restore the function of exhausted T cells and have been approved for the treatment of several different cancers (5–7). However, despite their durable therapeutic responses and mitigated side effects, only around 30% of patients on average exhibit a durable clinical benefit. In addition to the tumor microenvironment, recent research has emphasized the importance of tumor-draining lymph nodes (TDLNs) in priming and maintaining tumor-specific CD8 T cells, as well as enhancing CD8 T cell responses after PD-1 blockade (8, 9).

We and others recently identified a unique subset of virus-specific PD-1$^+$ TCF1$^+$ stem-like CD8 T cells that functions as resource cells to maintain virus-specific CD8 T cell immunity in the model of chronic lymphocytic choriomeningitis virus (LCMV) infection (10–12). These stem-like CD8 T cells sustain themselves by slow self-renewal and differentiate into a CX3CR1$^+$ transitory population and CD101$^+$ terminally exhausted CD8 T cells accompanied with antigen-driven proliferation (10–14). The stem-like CD8 T cells mainly reside in the lymphoid organs, while the more differentiated CD8 T cells are located in both lymphoid and nonlymphoid organs. Most importantly, the proliferative burst that is seen after PD-1-targeted therapy comes exclusively from the stem-like CD8 T cells. Furthermore, we recently showed that the stem-like CD8 T cells also proliferate and generate highly functional effector-like progeny cells upon combination therapy with PD-1 blockade and IL-2 (15). These results suggest that these PD-1$^+$ TCF1$^+$ stem-like CD8 T cells are critical for effective immunotherapy.

Stem-like CD8 T cells have also been identified in human and murine tumors (16–22). Similar to the results in chronically infected mice, stem-like CD8 TILs isolated from tumor-bearing mice can differentiate into terminally differentiated cells and exclusively respond to PD-1 pathway blockade. Correspondingly, approaches for increasing the

Significance

Recent studies in chronic viral infections and cancers have defined a population of PD-1$^+$TCF1$^+$ stem-like CD8 T cells. These self-renewing stem-like cells act as resource cells for maintaining T cell immunity under conditions of chronic antigen stimulation and also provide the proliferative burst after PD-1-targeted immunotherapy. In this study, we show that these key chronic resource CD8 T cells share similar phenotype, transcriptional profile, and biological functions in cancer and chronic viral infection. Interestingly, the PD-1$^+$TCF1$^+$ stem-like CD8 T cells are preferentially located in tertiary lymphoid structures (TLSs) in human lung cancer samples highlighting the importance of TLSs in providing a niche for the maintenance of this CD8 T cell population and more broadly for cancer immunotherapy.

Author contributions: S.J.I., R.C.O., S.S.R., and R.A. designed research; S.J.I., R.C.O., T.H.N., D.M., A.O.K., S.G., K.Y., and G.L.S. performed research; S.J.I., R.C.O., D.M., A.O.K., N.P., J.W.C., L.E.C., A.N.A.G., H.T.K., H.I.N., and R.A. analyzed data; and S.J.I., R.C.O., and R.A. wrote the paper.

Reviewers: D.C., IGM Biosciences; and P.R., Baylor College of Medicine.

The authors declare no competing interest.

[1]S.J.I. and R.C.O. contributed equally to this work.

[2]To whom correspondence may be addressed. Email: sejinim@skku.edu, ssramal@emory.edu, or rahmed@emory.edu.

This article contains supporting information online at https://www.pnas.org/lookup/suppl/doi:10.1073/pnas.2221985120/-/DCSupplemental.

Published October 2, 2023.

differentiation into TCF1$^+$ stem-like CD8 T cells such as the overexpression of transcription factor c-Myb, the genetic perturbation of histone demethylase LSD1, or the treatment of cyclophosphamide and vinorelbine led to the augmented therapeutic efficacy of PD-1-directed immunotherapy (23–25). Additionally, ectopic TCF1 expression or in vitro treatment with lactate augmented the efficacy of adoptive T cell therapy by promoting stem-like T cell differentiation (26, 27). It has been also shown that the presence of the TCF1$^+$ stem-like CD8 T cell subset is associated with the clinical outcome of checkpoint immunotherapies in melanoma and nonsmall lung cancer patients (19–22). However, it is unclear what are similarities and differences of exhausted CD8 T cell subsets between chronic viral infection and tumor and where stem-like CD8 T cells are specifically located within the tumor microenvironment. In this study, we compared the phenotypic, functional, and transcriptional characteristics of TCF1$^+$ stem-like and Tim-3$^+$ terminally differentiated CD8 TILs in murine and human cancers to the corresponding subsets in chronically infected mice as well as their anatomical locations.

Results

Identification of Stem-Like and Terminally Differentiated CD8 TIL Subsets in Solid Murine Tumors. To examine the phenotypic characteristics of tumor-specific CD8 TILs in solid murine tumors, we used melanoma (B16F10), lung carcinoma (LLC1), colon carcinoma (CT26), and prostatic adenocarcinoma (TRAMP-C2) models. The TILs were isolated at indicated time points when the tumors reached an area of approximately 1 cm^2. First, we observed that more than 80% of CD8 TILs in tumors expressed PD-1 (Fig. 1*A*). In addition, we found a distinct TCF1$^+$Tim-3$^-$ CD8 TIL subset among PD-1$^+$ CD8 TILs in all tumor models, but they were present at lower frequencies compared to those present in the spleen of LCMV-infected mice. These Tim-3$^-$PD-1$^+$ CD8 TILs completely lacked granzyme B expression. Furthermore, they showed lower PD-1 but higher CD73 expression than Tim-3$^+$PD-1$^+$ CD8 TILs, consistent with the phenotype of the corresponding stem-like CD8 T cell subset found in chronically infected mice.

We then examined the phenotype of tumor-specific CD8 T cells using a tetramer specific to the CT26 GP70$_{423\text{-}432}$ epitope in the CT26-bearing mice (Fig. 1*B*). We first confirmed that these tetramer$^+$ tumor-specific CD8 T cells were PD-1^{hi}. Furthermore, Tim-3$^-$ tumor-specific CD8 TILs highly expressed both TCF1 and CD73, while Tim-3$^+$ did not. By introducing the LCMV glycoprotein (GP) into both B16F10 and LLC1 tumor cell lines, we were able to examine tumor-specific T cell responses using LCMV GP-specific tetramers (Fig. 1*C*). In both B16F10-GP- and LLC1-GP-bearing mice, Tim3$^-$ tetramer$^+$ CD8 T cells were TCF1$^+$2B4$^-$, whereas Tim3$^+$ tumor-specific CD8 T cells exhibit a phenotype of TCF1$^-$2B4$^+$. It is worth emphasizing that the stem-like CD8 TIL phenotype in all three tumor models is consistent with the phenotype of LCMV-specific stem-like CD8 T cell subset in chronically infected mice. Taken together, these results confirm the phenotypic similarity of stem-like and terminally differentiated CD8 T cell subsets between chronic LCMV infection and solid murine tumors.

Proliferative Potential of Stem-Like CD8 T Cells Isolated from Tumor-Bearing Mice upon Antigen Reexposure. In mice chronically infected with LCMV, only stem-like CD8 T cells were shown to have proliferative potential after antigenic restimulation and PD-1 blockade (10). To investigate whether the proliferative potential would also be restricted to stem-like CD8 TILs, we isolated stem-like (Tim-3$^-$2B4$^-$ PD-1$^+$) and terminally differentiated (Tim-3$^+$2B4$^+$ PD-1$^+$) CD8 TILs from B16F10-GP-bearing mice. One thousand LCMV GP33/276-specific CD8 T cells of each subset were transferred into congenically distinct naive CD45.1 recipient mice separately (Fig. 2*A*). One day after the cell transfer, the recipient mice were rechallenged with the LCMV clone 13 (Cl-13) virus. In the blood, donor stem-like CD8 TILs expanded robustly and were maintained at least 14 days post infection (dpi), whereas terminally differentiated CD8 T cells did not expand (Fig. 2 *B* and *C*). Furthermore, over 1,000-fold more donor GP33/GP276-specific CD8 T cells were observed in the spleen of recipient mice given stem-like CD8 TILs compared to mice that received terminally differentiated CD8 TILs (Fig. 2 *D* and *E*). Stem-like CD8 TILs also gave rise to more cells than terminally differentiated CD8 TILs in the liver and lung. Interestingly, the donor Tim-3$^-$2B4$^-$ stem-like CD8 T cell subset gave rise to Tim-3$^+$2B4$^+$ effector progeny CD8 T cells after expansion, while donor terminally differentiated CD8 T cell subset maintained the Tim-3$^+$2B4$^+$ phenotype (Fig. 2*F*). This result confirms the precursor–progeny relationship of these two subsets and an exclusive proliferative potential of stem-like CD8 TILs in a murine solid tumor model similar to the relationship observed during chronic LCMV infection.

Similarities in Transcriptional Profiles of CD8 T Cell Subsets between Tumor and Chronic LCMV Infection. Next, we examined the transcriptional profile of stem-like and terminally differentiated CD8 TILs (Fig. 3). We isolated Tim-3$^-$2B4$^-$ PD-1$^+$ stem-like and Tim-3$^+$2B4$^+$ PD-1$^+$ terminally differentiated CD8 TILs from B16F10-GP-bearing mice and performed microarray analysis. This analysis revealed that stem-like and terminally differentiated CD8 TILs exhibited a similar gene signature to their corresponding subsets in chronically infected mice. For example, stem-like CD8 TILs had an overall lower expression of inhibitory receptors and higher expression of costimulatory molecules (Fig. 3*A*). In contrast to chronic LCMV infection, however, terminally differentiated CD8 TILs exhibited high expression of *Tnfrsf4* (OX40) and *Icos*. The expression pattern of chemokines and chemokine receptors was similar between chronic LCMV infection and tumor. Stem-like CD8 T cells in both models showed high expression of *Xcl1*, *Cxcl10*, *Cxcl11*, *Cxcr4*, and *Cxcr5*, whereas terminally differentiated CD8 T cells showed high expression of *Ccl3*, *Ccl4*, *Ccl5*, *Ccr5*, and *Cxcr6*, which are associated with local inflammation (28).

Of interest, the *Cxcr5* transcript was present in stem-like CD8 T cells from both the tumor and LCMV models. CXCR5 was used as a phenotypic marker for identifying the stem-like CD8 T cells in the LCMV chronic infection model (10, 11). However, TILs usually do not stain positive for CXCR5. The reason for this is that the collagenase treatment used to isolate T cells from the tumor digests the CXCR5 molecule from the cell surface. The effect of collagenase treatment in removing CXCR5 is shown in Fig. 4 where we treated LCMV-specific CD8 T cells with collagenase that resulted in lack of staining with CXCR5 antibody.

We also confirmed higher *Eomes* and lower *Tbx21* (T-bet) expression in stem-like CD8 TILs, consistent with the results in chronically infected mice. However, both subsets showed higher expression of these transcription factors compared to naive CD8 T cells. *Tox*, a transcription factor known to regulate T cell exhaustion (29–31), was also highly expressed in both subsets of CD8 TILs. *Id2* and *Prdm1* (Blimp1) were selectively expressed in terminally differentiated CD8 TILs, while *Plagl1*, *Bcl6*, *Id3*, *Tcf7*, and *Foxo1* were highly expressed in stem-like CD8 TILs. Additionally, stem-like CD8 TILs showed higher expression of genes related to the self-renewal of

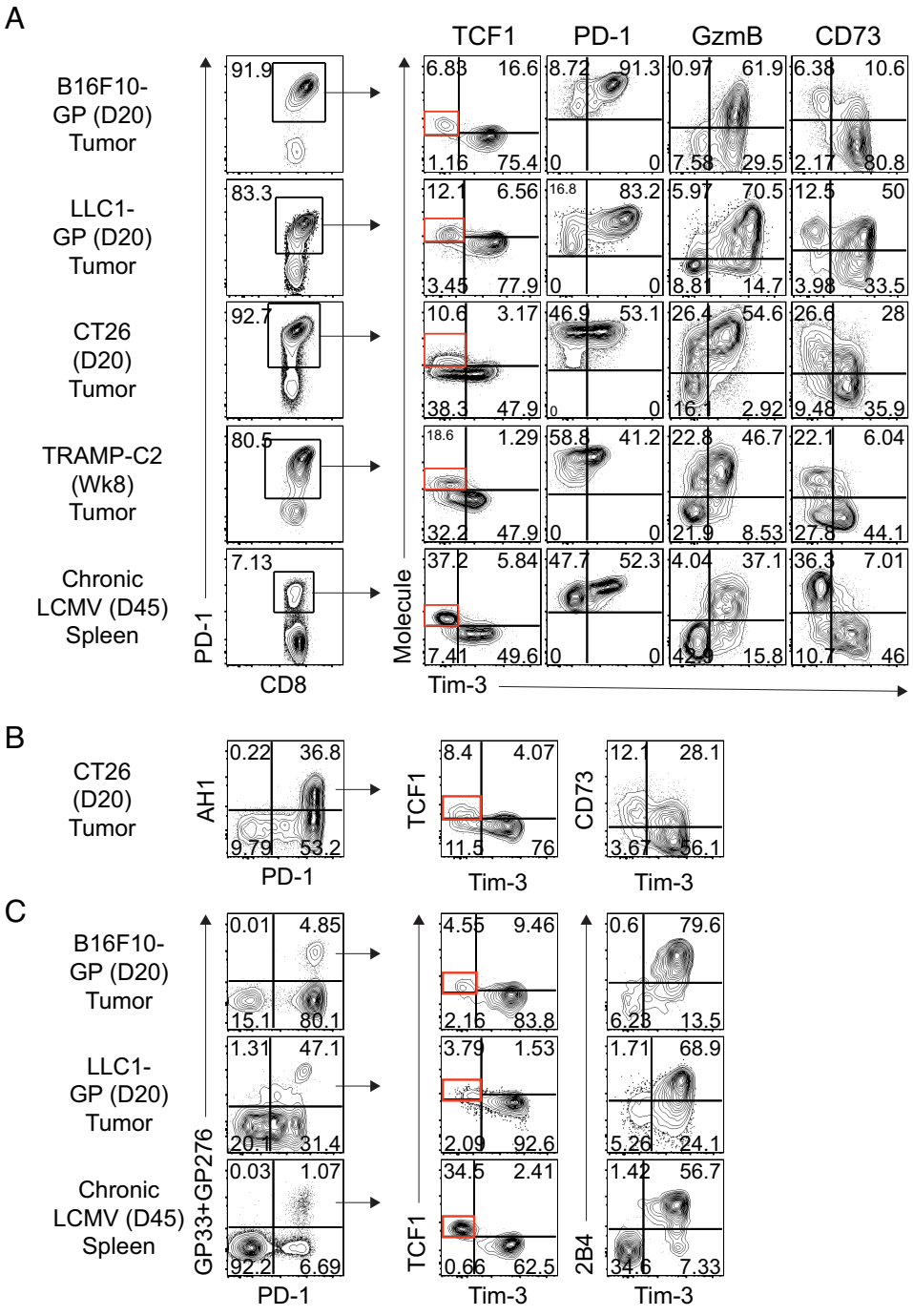

Fig. 1. Identification of stem-like and terminally differentiated CD8 TIL subsets in solid murine tumors. Phenotypic analysis of PD-1$^+$ cells (*A*) and tumor-specific tetramer-positive CD8 T cells (*B* and *C*) in the indicated tumors and the spleen of tumor-bearing mice and chronically LCMV-infected mice, respectively, at the indicated time points. Data are representative of three independent experiments (n = 5/experiment).

hematopoietic stem cells and cytokine genes such as *Il2* and *Tnf*. In comparison, terminally differentiated CD8 TILs exhibited higher expression of effector genes like *Gzma*, *Gzmb*, *Prf1*, and *Ifng*. The overlap in gene signature of chronic LCMV-derived and tumor-derived CD8 T cell subsets was also revealed by gene set enrichment analysis (GSEA) (Fig. 3*C*).

We next analyzed the enriched Reactome pathways in two CD8 T cell subsets of each model and compared them between two models. Translation-, IFNαβ signaling-, IFNγ signaling-, and cell-cell communication-related genes were enriched in stem-like CD8 T cells from both chronically infected and tumor-bearing mice (Fig. 3*D*). In contrast, proliferation-, apoptosis-, and cholesterol biosynthesis–related genes were commonly enriched in terminally exhausted CD8 T cells. Taken together, these comparisons suggest that stem-like and terminally differentiated CD8 TILs primarily share transcriptional profiles with their respective subsets present in chronically infected mice.

Differences in Transcriptional Profiles of CD8 T Cell Subsets between Tumor and Chronic LCMV Infection. The above results show the striking similarities between the CD8 T cell subsets in tumor models and chronic LCMV infection. However, we also

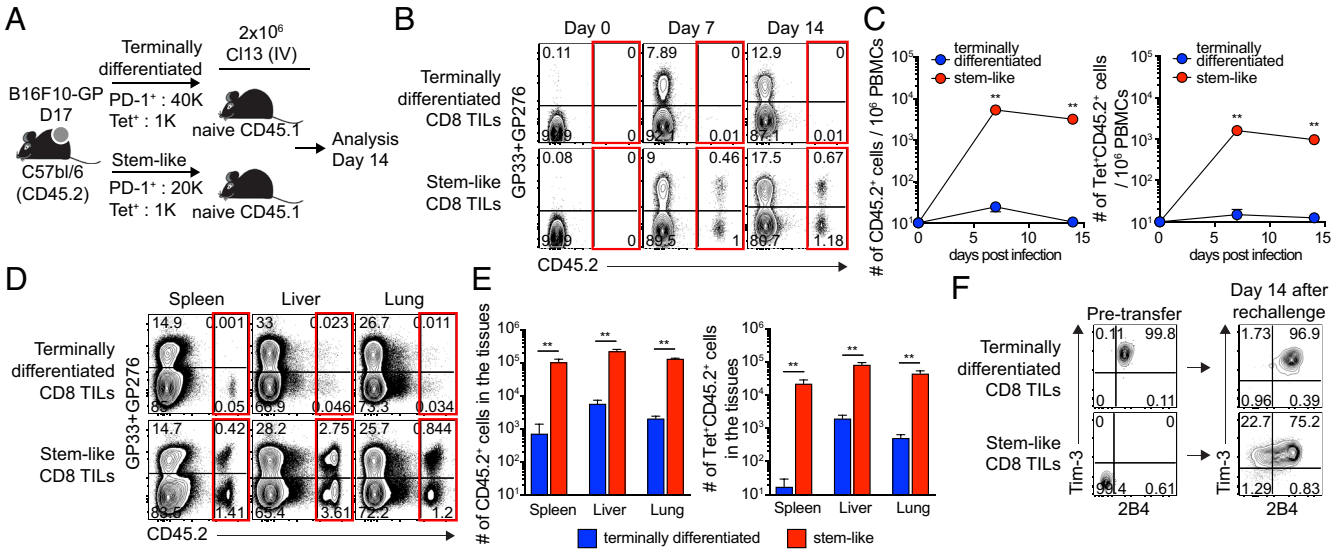

Fig. 2. Proliferative potential of stem-like CD8 T cells isolated from tumor-bearing mice upon antigen reexposure. (*A*) Experimental setup illustrating transfer of congenically marked Tim-3$^+$2B4$^+$ PD-1$^+$ (terminally differentiated) and Tim-3$^-$2B4$^-$ PD-1$^+$ (stem-like) CD8 T cells isolated from B16F10-GP-bearing mice (day 17) into naive Ly5.1 recipient mice, followed by LCMV Cl-13 challenge. (*B* and *C*) Representative FACS plots (*B*) and kinetics of total donor cells and donor GP33/GP276-specific CD8 T cells (*C*) in the blood (*D* and *E*) Representative FACS plots (*D*) and the number of total donor cells and donor GP33/GP276-specific CD8 T cells (*E*) in the tissues at day 14 post the challenge. (*F*) Phenotypic analysis of donor CD8 TIL subsets before and after the transfer followed by Cl-13 challenge. Data were representative of two independent experiments (n = 4/experiment). Graph shows the mean and SEM. Student's *t* test, where $^{**}P < 0.01$.

noted some differences. Both stem-like and terminally differentiated CD8 TILs were enriched in genes associated with the cell cycle and apoptosis compared to their counterparts in chronically infected mice (Fig. 5). The enrichment of cell cycle–related genes was consistent with higher Ki-67 expression of both subsets in tumor-bearing mice (*SI Appendix*, Fig. S1*A*). When we examined the

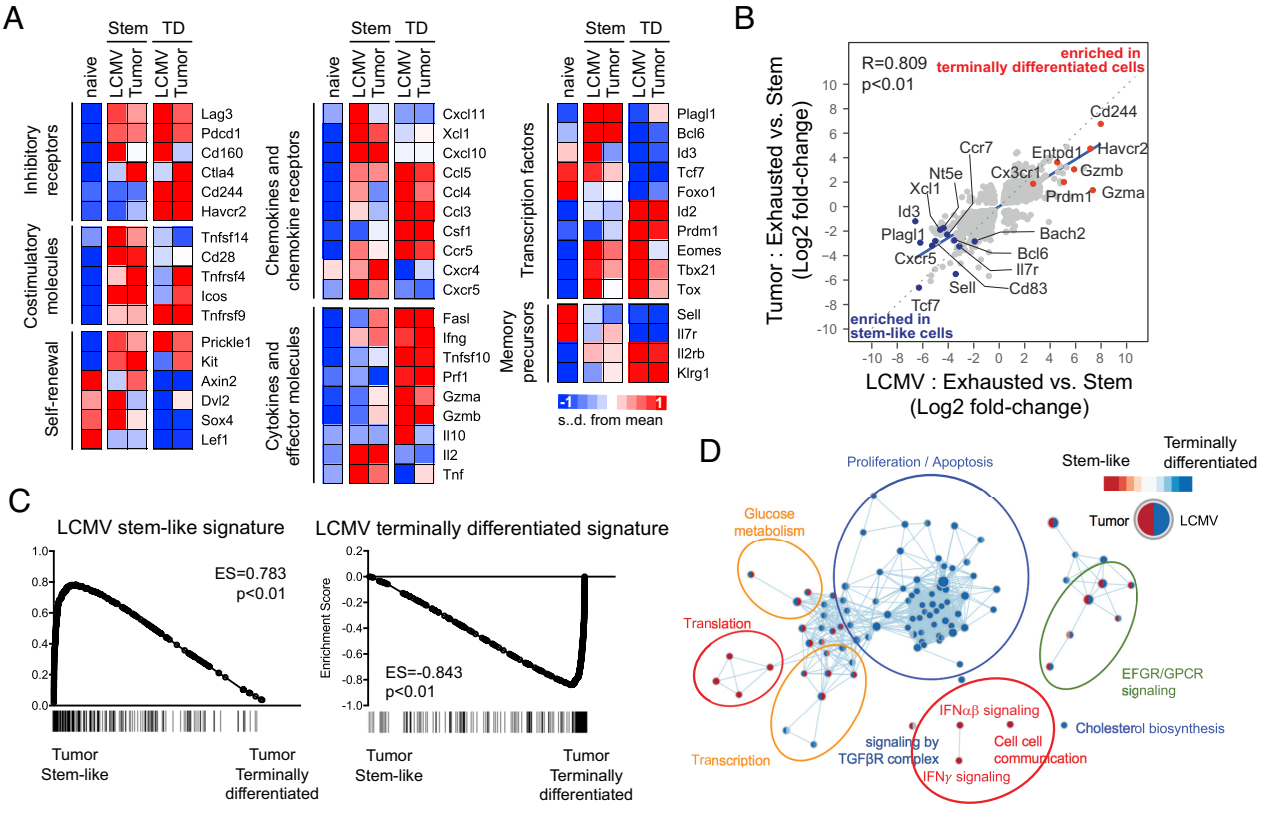

Fig. 3. Similarities in transcriptional profiles of CD8 T cell subsets between tumor and chronic LCMV infection. Tim-3$^-$2B4$^-$ PD-1$^+$ stem-like and Tim-3$^+$2B4$^+$ PD-1$^+$ terminally differentiated CD8 TILs were isolated from B16F10-GP tumor-bearing mice at day 19 post inoculation. Affymetrix microarray was performed to examine the transcriptome of isolated CD8 TILs, then they were compared with that of two CD8 T cell subsets obtained from mice chronically infected with LCMV (GSE84105) (*A*) Heat map displaying the relative expression of genes in naive (CD44^{lo}CD127$^+$CD62L$^+$) CD8 T cells from uninfected mice, two CD8 TIL subsets from tumor-bearing mice and two CD8 T cell subsets from chronically infected mice. (*B*) A scatter plot showing differentially expressed genes with twofold cutoff (in addition to the adjusted *P*-value < 0.05 cutoff) between two CD8 T cell subsets in chronically infected mice (*X* axis) and tumor-bearing mice (*Y* axis). (*C*) GSEA for identifying specific gene signatures of two murine CD8 TIL subsets compared to gene signatures of LCMV stem-like and exhausted CD8 T cells. (*D*) Cytoscape network analysis for identifying enriched Reactome pathways in each CD8 T cell subset.

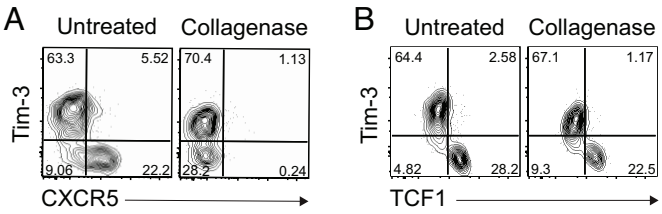

Fig. 4. Digestion of CXCR5 molecules on the stem-like CD8 T cells by collagenase treatment. Representative FACS plots of CXCR5 (*A*) and TCF1 (*B*) versus Tim-3 expression on GP33-specific CD8 T cells in the spleen of chronically LCMV-infected mice according to the treatment of the collagenase. Data were representative of two independent experiments (n = 4/experiment).

kinetics of Ki-67 expression in CD8 T cells during the course of LCMV infection, both CD8 T cell subsets were highly proliferating at 8 dpi (*SI Appendix*, Fig. S1*B*). After that, Ki-67 expression gradually declined, and the stem-like subset became quiescent by 28 dpi, while a fraction of terminally differentiated CD8 T cells still expressed it. Therefore, the enrichment of cell cycle- and apoptosis-related genes in the subsets of CD8 TILs was likely due to the different time points of examination (day 20 versus day 45) after tumor inoculation and viral infection, respectively.

Genes related to hypoxia were also specifically up-regulated in both subsets of CD8 TILs, suggesting that low oxygen level in the tumor microenvironment induces changes in gene expression profiles in CD8 TILs irrespective of the T cell state (Fig. 5). In contrast, genes associated with IFNαβ signaling were up-regulated more in CD8 T cells from LCMV-infected mice than in the cells from tumor-bearing mice. It is well documented that type I IFNs (IFN-Is) are induced at high levels during viral infections, while the production of IFN-Is is much lower in a tumor setting (32, 33). These results suggest that the local microenvironment is commonly involved in the regulation of gene expression profiles irrespective of CD8 T cell subsets.

Furthermore, the comparison of enriched Reactome pathways between the two CD8 T cell subsets of each model showed that genes involved in glucose metabolism and transcription were highly expressed only in the stem-like CD8 T cells from chronically infected mice (Fig. 3*D*). At the same time, epidermal growth factor receptor (EGFR) and G-protein-coupled receptor (GPCR) signaling pathways were enriched in the stem-like CD8 TILs, suggesting unique features of the stem-like CD8 T cell subset between chronic viral infection and cancer. However, we still found no significant enrichment of the mTOR pathway (ES = 0.2, $P = 0.42$) comparing these cells suggesting a similar level of mTOR signaling in the TCF1$^+$PD1$^+$ cells in cancer and LCMV.

Therefore, despite the common transcriptional signatures for the lineage differentiation into stem-like and terminally differentiated CD8 T cells in both chronic viral infection and cancer, the individual microenvironment still regulates gene expression profiles.

Characteristics of TCF1$^+$PD-1$^+$ CD8 TILs in Human NSCLC Patients. We next examined the phenotypic characteristics of CD8 TILs isolated from stage I–IV nonsmall cell lung cancer (NSCLC) patients (Fig. 6*A* and *SI Appendix*, Table S1). We found that around 80% of tumor-infiltrating CD8 T cells, ranging from 50 to 95%, expressed PD-1 (Fig. 6*B*). In addition, a considerable population of Tim-3$^+$PD-1$^+$ CD8 TILs, varying from 5 to 40% of CD8 TILs, was observed in 12 out of 16 patients (Fig. 6*B*) and the frequency of Tim-3$^+$PD-1$^+$ CD8 T cells was positively correlated to a population of total PD-1$^+$ CD8 T cells (Fig. 6*C*). More importantly, there was a significant linear correlation between the frequency of Tim-3$^+$PD-1$^+$ CD8 TILs and proliferating (Ki-67$^+$) PD-1$^+$ CD8 T cells (Fig. 6*D*). In accordance with our results in murine tumor models and HNSCC patients (18), Tim-3$^-$PD-1$^+$ CD8 TILs were enriched with TCF1$^+$ cells compared to Tim-3$^+$PD-1$^+$ CD8 TILs in NSCLC patients (Fig. 6*E*). It is noteworthy that both TCF1$^+$ and TCF1$^-$ subsets were observed within the Tim-3$^-$PD-1$^+$ CD8 T cell population. Interestingly, we have also observed the presence of TCF1$^-$Tim-3$^-$ PD-1$^+$ CD8 T cells in patients with head and neck cancer using HPV-specific tetramers (18) as well as in kidney cancer patients and TRAMPC1-GP tumor-bearing mice (8). These findings indicate additional heterogeneity within the TCF1$^-$ CD8 TIL population. It is possible that TCF1$^-$Tim-3$^-$ PD-1$^+$ CD8 T cells may represent an early transitional population during the transition from TCF1$^+$Tim-3$^-$ cells to TCF1$^-$Tim-3$^+$ cells.

We also found that Tim-3$^+$PD-1$^+$ CD8 TILs exhibited higher expression of inhibitory receptors, PD-1 and CD39, and a cytolytic molecule, granzyme B (Fig. 6 *F* and *G*). It is noteworthy that TCF1$^+$Tim-3$^-$ CD8 TILs were largely quiescent (Ki-67$^-$) in NSCLC patients, while Tim-3$^+$ CD8 TILs were actively proliferating, as evidenced by the expression of Ki-67 (Fig. 6 *G* and *H*).

CD28 costimulatory signals are important for efficient PD-1-directed immunotherapy (34, 35). The proliferative burst of effector CD8 cells from the stem-like cells after PD-1 blockade requires not only removing the PD-1 inhibitory brake but also providing costimulatory signals from CD28 (34). In this context,

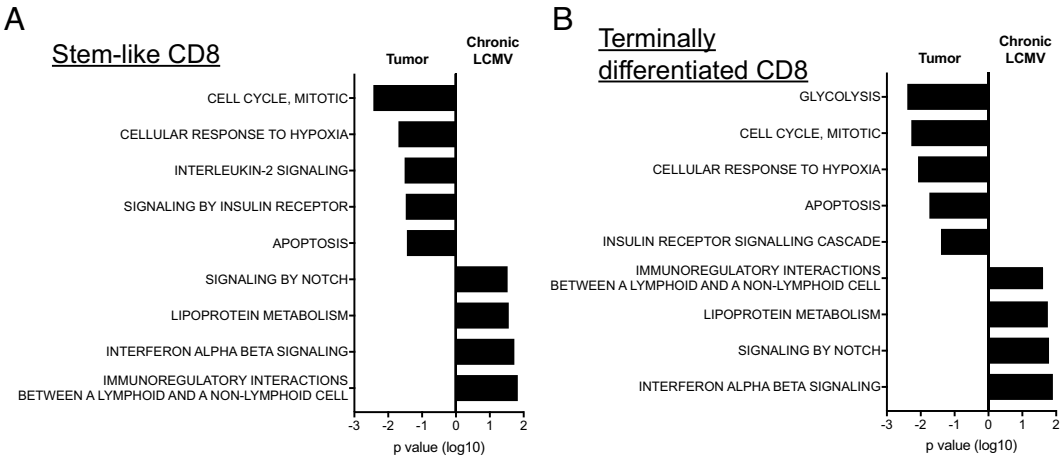

Fig. 5. Differences in transcriptional profiles of CD8 T cell subsets between tumor and chronic LCMV infection. Affymetrix microarray was performed as described in Fig. 3. Enriched Reactome pathways in Tim-3$^-$2B4$^-$ stem-like (*A*) and Tim-3$^+$2B4$^+$ terminally differentiated CD8 T cells (*B*) were compared between tumor and chronic LCMV models.

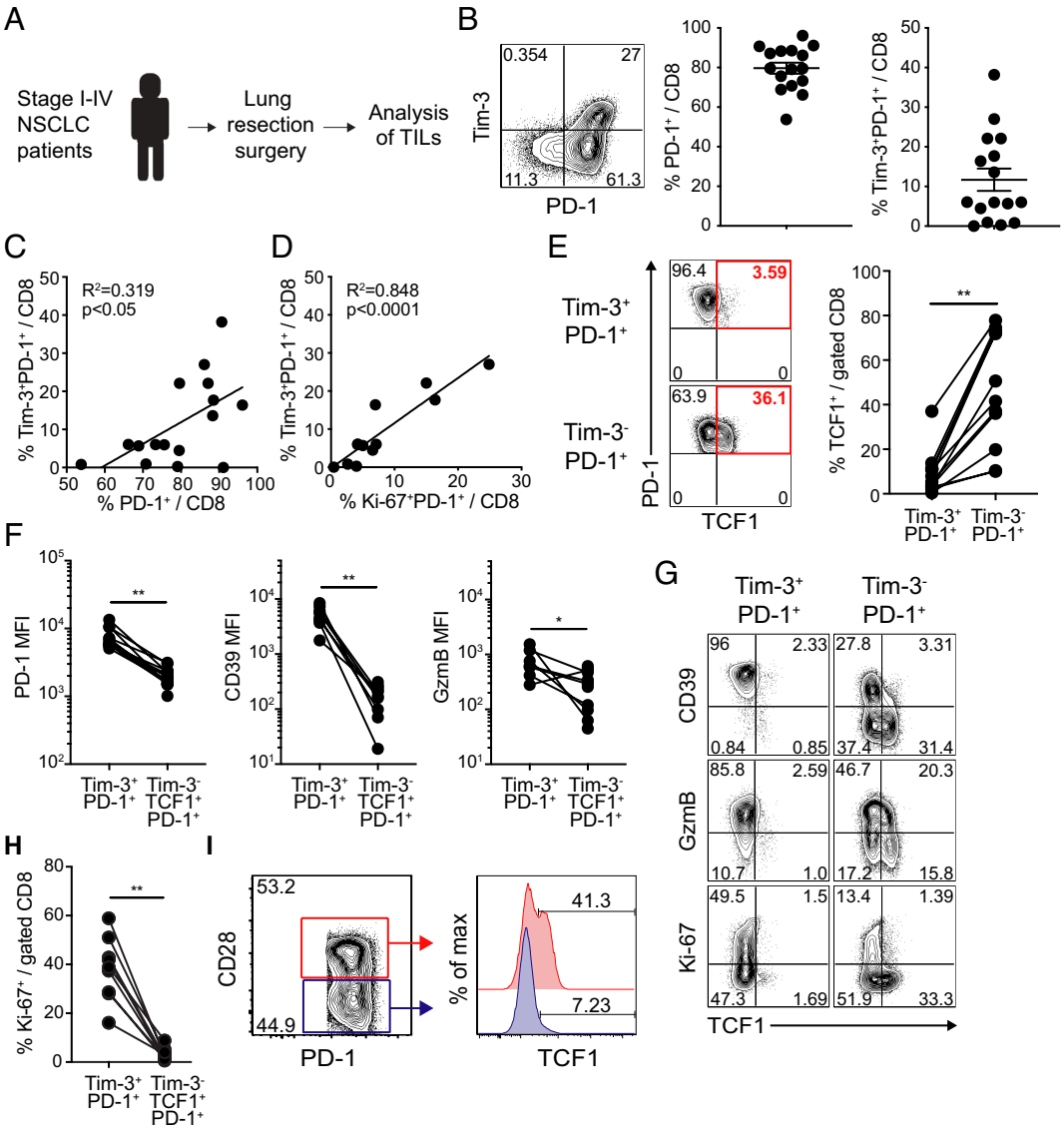

Fig. 6. Phenotypic characterization of TCF1$^+$Tim-3$^-$ CD8 TILs in human NSCLC patients. (*A*) Overview of study design. (*B*) Representative FACS plots of PD-1 and Tim-3 expression on CD8 TILs and frequency of PD-1$^+$ and Tim-3$^+$PD-1$^+$ CD8 cells among total CD8 TILs in NSCLC tumors. (*C* and *D*) Correlation of the frequency of Tim-3$^+$PD-1$^+$ CD8 cells with that of PD-1$^+$ CD8 cells (*C*) and Ki-67$^+$PD-1$^+$ CD8 cells (*D*) among total CD8 TILs. (*E*) Frequency of TCF1$^+$ cells in Tim-3$^+$PD-1$^+$ and Tim-3$^-$PD-1$^+$ CD8 TILs. (*F* and *G*) MFI of PD-1, CD39, and granzyme B expression (*F*) in Tim-3$^+$PD-1$^+$ and Tim-3$^-$TCF1$^+$PD-1$^+$ CD8 TILs and representative FACS plots including Ki-67 expression (*G*). (*H*) Frequency of Ki-67$^+$ cells in Tim-3$^+$PD-1$^+$ and Tim-3$^-$TCF1$^+$PD-1$^+$ CD8 TILs. (*I*) Representative FACS plots of the frequency of TCF1$^+$ cells in CD28$^+$ and CD28$^-$ PD-1$^+$ CD8 TILs. Graph shows the mean and SEM. Paired Student's *t* test, where $^{**}P < 0.01$; $^{*}P < 0.05$.

it is worth noting that CD28$^+$ CD8 TILs possess more TCF1$^+$ cells than CD28$^-$ CD8 TILs in human lung cancers (Fig. 6*I*). Thus, CD28 is a critical marker of functional TCF1$^+$ stem-like CD8 T cells in both chronic viral infection and cancer.

We also examined the transcriptional profiles of CD8 TILs isolated from human NSCLC patients by RNA sequencing. We used CD28 expression to enrich for stem-like cells among Tim-3$^-$PD-1$^+$ CD8 TILs and isolated stem-like CD28$^+$Tim-3$^-$PD-1$^+$ CD8 TILs and terminally differentiated Tim-3$^+$PD-1$^+$ CD8 TILs from NSCLC tumors (*SI Appendix*, Fig. S2). Transcriptional profiling revealed that stem-like and terminally differentiated CD8 T cell subsets isolated from NSCLC patients had distinct gene signatures (Fig. 7 *A*–*C*). For example, there was a trend that stem-like human CD8 TILs exhibited higher expression of costimulatory molecules, memory-related genes, and Toll-like receptors (TLRs), whereas terminally differentiated human CD8 TILs highly expressed inhibitory receptors, effector genes, inflammatory chemokines, and *MKI67*. Transcription factors related to the differentiation into stem-like CD8 T cells such as *BCL6*, *TCF7* (encoding TCF1), *LEF1*, and *EOMES* were also enriched in stem-like CD8 TILs. Consistently (29–31), higher *TOX* expression was observed in both subsets of CD8 TILs than naive CD8 T cells.

GSEA of Reactome pathways revealed that translation, TCR signaling, NF-kB and MAPK activation by TLR, and TRIF-mediated TLR3 signaling were enriched in stem-like TILs, while the cell cycle pathway was enriched in terminally differentiated TILs (Fig. 7*D*). We also observed an enrichment of stem-like and terminally differentiated CD8 T cell signatures that were previously seen in chronically infected mice in the corresponding human TIL subsets (Fig. 7*E*). Collectively, these results support that stem-like CD8 TILs also exist in human lung cancers and they exhibit similar phenotypic and transcriptional profiles to corresponding CD8 T cell subsets found in chronically infected mice and tumor-bearing mice.

Localization of Stem-Like CD8 T cells in Chronically Infected Mice and Human Tumors in the Lung. The presence of stem-like CD8 T cells in the tumor microenvironment (TME) raised questions about the specific location of stem-like CD8 T cells

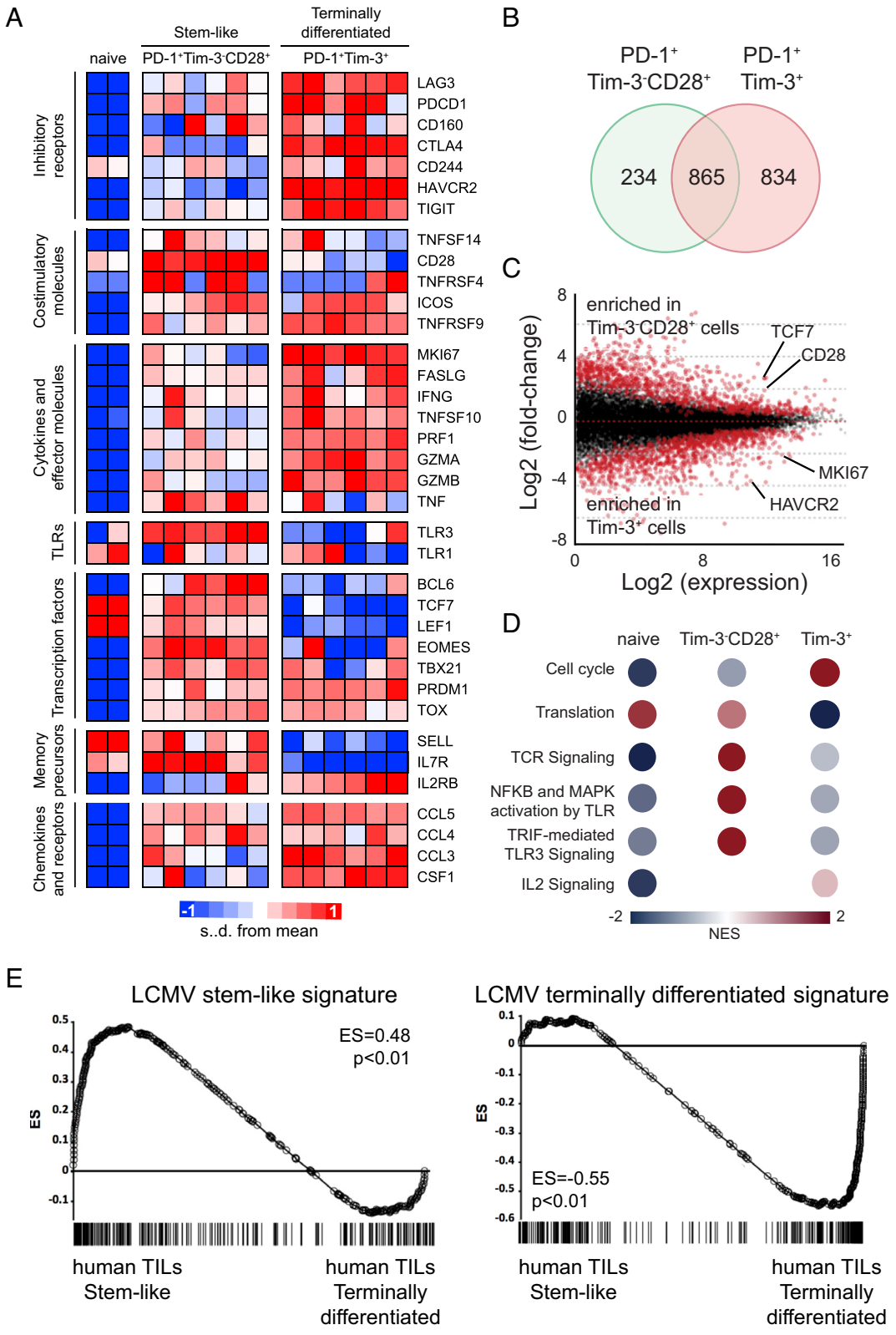

Fig. 7. Transcriptional profiles of two CD8 TIL subsets isolated from NSCLC patients. Tim-3$^-$CD28$^+$ PD-1$^+$ stem-like and Tim-3$^+$ PD-1$^+$ terminally differentiated CD8 TILs were isolated from NSCLC patients. RNA-seq was performed to examine the transcriptome of isolated CD8 TILs. (*A*) Heat map displaying the relative expression of genes in naive (CCR7$^+$CD45RA$^+$CD58$^-$CD95$^-$) CD8 T cells from a healthy subject and a NSCLC patient and two CD8 TIL subsets from six NSCLC patients. (*B*) DEGs in the stem-like and terminally differentiated CD8 T cells compared to naive CD8 T cells. Venn diagram illustrates the overlap in stem-like and exhausted cells among DEGs. (*C*) Scatter plot of log2 fold-change between stem-like and terminally differentiated CD8 T cells versus mean average read counts. Red indicates genes that were significantly different (adjusted *P*-value < 0.01). (*D*) Reactome pathways which were enriched in each CD8 T cell subset compared to other two subsets. NES, normalized enriched score. (*E*) GSEA for identifying specific gene signatures of two human CD8 TIL subsets compared to gene signatures of LCMV stem-like and terminally differentiated CD8 T cells.

and their spatial relationships with other immune cells in the TME. We have previously observed the enrichment of stem-like CD8 T cells in lymphoid tissues such as the spleen and lymph nodes in chronically infected mice (36). These observations suggest that stem-like CD8 T cells may be enriched in lymphoid aggregates like TLSs in the TME of human tumors. To further characterize the location of stem-like CD8 T cells, we examined the spatial organization of TCF1$^+$PD-1$^+$ and Tim-3$^+$PD-1$^+$ CD8 T cells within the spleens of chronically infected mice. We first confirmed that most viral infected cells were primarily localized in the red pulp, whereas viral antigens were rarely observed in the white pulp of the spleen of chronically infected mice (*SI Appendix*, Fig. S3*A*). We next used intravascular labeling to distinguish cells in the blood-accessible red pulp from those situated in the white pulp, the lymphoid compartment of the spleen (*SI Appendix*, Fig. S3*B*). TCF1$^+$PD-1$^+$ and Tim-3$^+$PD-1$^+$ antigen-specific cells were clearly located in distinct compartments within the spleen. Majority of the TCF1$^+$PD-1$^+$ cells were located in the lymphoid compartment (white pulp), while the terminally differentiated Tim-3$^+$PD-1$^+$ cells were predominantly in the red pulp of the spleen (*SI Appendix*, Fig. S3 *C–E*).

To determine where stem-like CD8 T cells were located in the TME of human tumors in the lung, we examined TCF1$^+$PD-1$^+$ and TCF1$^-$PD-1$^+$ CD8 T cell subsets in formalin-fixed paraffin-embedded tumor sections from surgical resection samples from cancer patients using multiplex immunohistochemistry (Fig. 8*A*). Regions of tumor parenchyma marked by cytokeratin and nuclear features were identified and differentiated from stromal areas lacking cytokeratin expression (regions indicated by orange dashes in Figs. 8 *D–F* and 9 *A–C*). Infiltration of the tumor by PD-1$^+$ and stem-like TCF1$^+$PD-1$^+$ CD8 T cells was variable in the different tumors evaluated. Within the tumor parenchyma (marked by positive cytokeratin staining), TCF1$^+$PD-1$^+$ CD8 T cells were less prominent and rare (Fig. 8 *B*, *D–F*). However, TCF1$^-$PD-1$^+$ CD8 T cells were easily identified within the tumor parenchyma (Fig. 8*C*) and in the stromal regions throughout the tumor bed (Fig. 8 *D–F*). These observations suggest that the distribution pattern of stem-like CD8 T cells is distinct from TCF1$^-$PD-1$^+$ CD8 T cells in the TME.

Based on our observations that TCF1$^+$PD-1$^+$ cells are preferentially located in lymphoid compartments in tissues (18, 36), we hypothesized that stem-like CD8 T cells reside in tertiary lymphoid structures (TLSs) within tumors. First, we evaluated the presence and composition of lymphoid aggregates in the tumor bed. We identified lymphoid aggregates that were mainly composed of T cells or B cells and other aggregates that were composed of tight clusters of B and T cells indicative of TLSs (Fig. 9 *A–C*). Discrete lymphoid aggregates were identified in 11 out of the 13 samples that we analyzed and the number of aggregates ranged from 0.16/mm^2 to 1.36/mm^2. Two samples had small T cell-only aggregates (0.16/mm^2 and 0.27/mm^2).

Nine out of 13 (69.2%) of the tumors examined had aggregates of T and B cells corresponding to TLSs that ranged from 0.19/mm^2 to 1.1/mm^2. There were no significant differences in the number of TLSs per mm^2 between primary and metastatic tumors or based on tumor grade (i.e. stage of differentiation), tumor stage, and sex. TLSs were identified in tumors at all three stages of tumor differentiation, with well-differentiated tumors showing morphologic and architectural features consistent with the cell lineage of origin, moderately-differentiated tumors that had morphologic features similar to the cells of origin but with a component of tumor that lacked the classic features of the cells of origin, and poorly-differentiated tumors that lacked features distinctive of the cell lineage of origin. The tumors that lacked TLSs (a mixture of T and B cells) were all moderately-differentiated tumors. TLSs with discernable T and B cell-like zones were present in all nine samples that had TLSs. TLSs with discernable T and B cell-like areas accounted for between 5% and 48% of the TLSs per mm^2. The TLSs were present in the stromal regions within and around the tumor bed.

To further determine whether the stem-like CD8 T cells were preferentially located in TLSs, we quantified TCF1$^-$PD-1$^+$ and stem-like TCF1$^+$PD-1$^+$ CD8$^+$ cells in the tumor parenchyma (ITL) and in TLSs within the tumor (iTLS), at the periphery of the tumor (pTLS), and adjacent to the tumor (aTLS). In the four tumor samples that did not have TLSs, TCF1$^+$PD-1$^+$ CD8$^+$ cells were rare and difficult to identify. For the samples that had TLSs, TCF1$^+$PD-1$^+$ CD8$^+$ cells were identified in the TLSs that were within and around the tumor (iTLS, pTLS, and aTLS; Figs. 8 *B*, *D–F* and 9 *A–C*). Additionally, spatial map analysis computing the distance from the nearest TCF1$^+$PD-1$^+$ CD8 T cell to each CD4 T cell or B cell showed that the TCF1$^+$PD-1$^+$ CD8 T cells were closer to CD4 T cells than B cells in the TLSs (Fig. 9*D*), suggesting the preferential clustering of stem-like CD8 T cells with CD4 T cells. Taken together, these results show that stem-like CD8 T cells preferentially cluster in TLSs and stay away from the tumor parenchyma.

Discussion

In this study, we compared phenotypic and transcriptional profiles of CD8 TILs in solid murine tumors and human NSCLC to those in the model of chronic LCMV infection. In line with the findings from the chronic LCMV infection, these stem-like cells in the murine tumor model exclusively proliferated and differentiated into effector-like cells following antigenic restimulation. Of note, we showed that TCF1$^+$ stem-like CD8 T cells in human lung tumors were mainly observed in TLS in the stromal areas and not within the tumor parenchyma.

One of the common features of stem-like CD8 T cells among chronically infected mice, tumor-bearing mice, and human cancer patients was the enrichment of genes associated with translation, including ribosomal proteins and ribosomal subunits. It is well known that the translational machinery genes that encode specific ribosomal proteins possess the sequence of 5′ terminal oligopyrimidine tracts (TOP) (37), and mTOR stimulates the translation of TOP mRNA (38, 39). Although persistent antigenic stimulation during chronic LCMV infection compromised AKT and mTOR activation (40), we have previously observed higher mTOR activation of stem-like CD8 T cells compared to terminally differentiated CD8 T cells in mice chronically infected with LCMV (10). Of interest, although PD-1 pathway blockade increased mTOR activity in CD8 T cells during chronic LCMV infection, the therapeutic effect of anti-PD-L1 antibodies was abrogated in mice that were also treated with rapamycin, an mTOR inhibitor (40). Similarly, Ando et al. recently found that a cell-intrinsic mTOR signaling play a role in the differentiation of stem-like CD8 T cells into Tim-3$^+$ terminally differentiated T cells (41). Therefore, mTOR inhibition prior to PD-1 blockade augmented its therapeutic efficacy, while simultaneous treatment abolished the effect of PD-1 blockade. These results highlight the importance of mTOR signaling in the proliferative potential of stem-like CD8 T cells.

IFN-related genes were expressed at higher levels in CD8 T cells from chronically infected mice compared to CD8 T cells from tumor-bearing mice, suggesting the influence of the specific microenvironment (Fig. 5). Interestingly, between the two CD8 T cell subsets, there was greater enrichment of IFN-related genes in the stem-like subset compared to the more differentiated subset

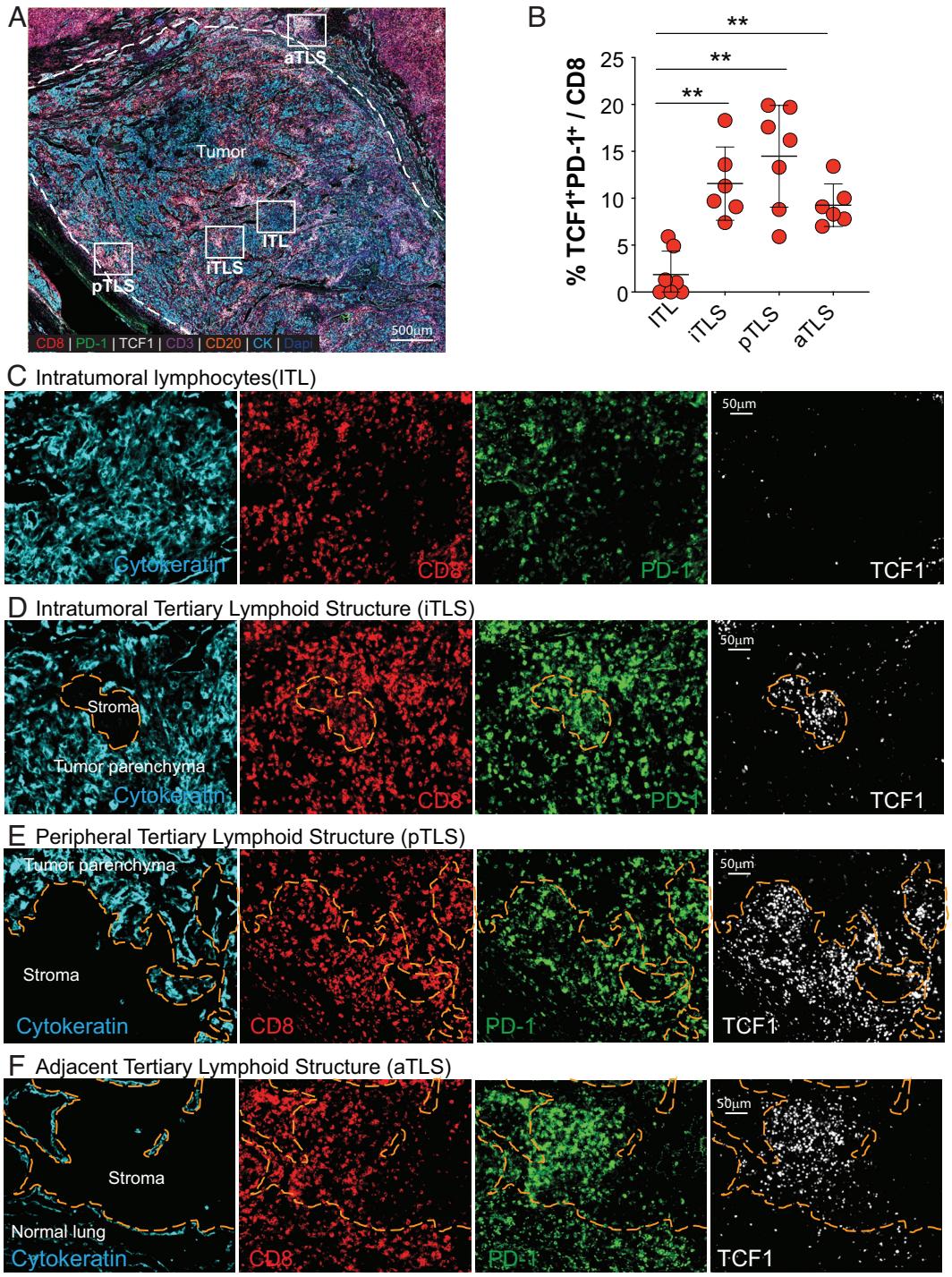

Fig. 8. Spatial location of stem-like CD8 T cells in primary and metastatic human tumors in the lung. (*A*) Representative area of a pleomorphic carcinoma of the lung. Areas corresponding to the tumor parenchyma containing intratumoral lymphocytes (ITL), tertiary lymphoid structures in the stroma within the tumor bed (iTLS), at the periphery of the tumor (pTLS), and adjacent to the tumor (aTLS) are designated by the white squares. (*B*) Summary graph showing the number and frequency of $TCF1^+PD\text{-}1^+$ CD8 T cells in indicated areas in (*A*) (n = 7). Horizontal line indicates mean and error bars represent SD. Paired Student's *t* test, $^{**}P < 0.01$; $^{*}P < 0.05$. (*C–F*) Representative areas of ITL, iTLS, pTLS, and aTLS showing the presence and distribution of $CD8^+$, $PD\text{-}1^+$, and $TCF1^+$ cells. Orange dashed region marks the stromal region.

and this trend was seen in CD8 T cells from both chronically infected or tumor-bearing mice (Fig. 3*D*). Earlier studies have shown that IFNα4, IFNα6, and IFNα9 significantly inhibited the proliferation of CD8 T cells in the acute viral infection model (42). Additionally, it has been reported that IFN-I has antiproliferative effects in a STAT1- and IL-27-dependent manner during chronic LCMV infection (43). Taken together, it is possible that IFN-I mediates the quiescence of stem-like CD8 T cell subset by inhibiting their proliferation and differentiation in the microenvironment of persistent antigenic stimulation.

When comparing T cell responses in various models of chronic infection and tumors, it is important to consider how the different temporal aspects of these models might influence the properties of the CD8 T cells. As summarized in *SI Appendix*, Table S2, PD-1 expression is high on all subsets of CD8 T cells, suggesting that they are seeing antigen in vivo, irrespective of the time or whether it was

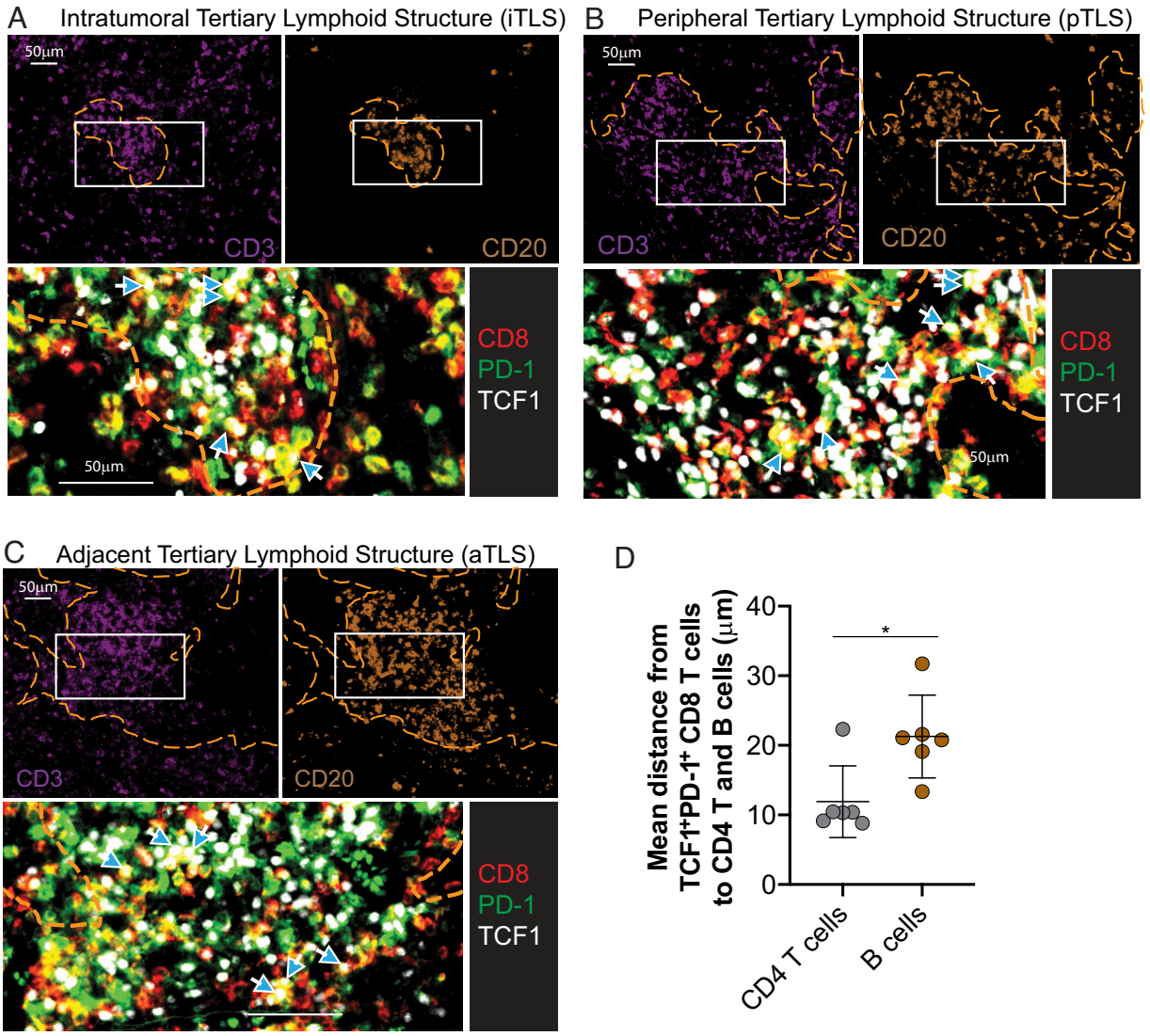

Fig. 9. Proximity of CD4 T cells and B cells to stem-like CD8 T cells in tumors. (*A–C*) Location of stem-like CD8 T cells in relation to B cell and CD4 T cell zones within the indicated TLSs from the pleomorphic carcinoma. (*D*) Summary plot showing the distance from the nearest stem-like CD8 T cells to each CD4 T cell ($CD3^+/CD8^-/CD20^-$) or B cell ($CD20^+$) from six different tumors. Graph shows the mean and SD. Paired Student's *t* test, where $*P < 0.05$.

viral versus tumor or murine versus human. Furthermore, TCF1 denotes the stem-like or Tpex CD8 T cells under all three conditions and is typically not expressed by the more differentiated and exhausted CD8 T cell subsets. In contrast, Ki-67 expression shows striking changes as a function of time and this is particularly evident for the stem-like CD8 T cell population. These $PD\text{-}1^+TCF1^+$ CD8 T cells are Ki-67 positive and undergoing proliferation during the early stages (first 2 to 3 wk) in both mouse tumor and chronic infection models but then their proliferation starts slowing down over time. The mouse chronic LCMV model allows us to monitor the stem-like CD8 T cells for extended periods and at later time points (> day 30 to 60), these Tpex cells are mostly quiescent. This quiescent feature of the stem-like T cell subset is also observed in TILs from NSCLC patients (Fig. 6 *G* and *H*) and has been reported in other human cancers (16, 18). In a recent study, we demonstrated that TGF-β up-regulated the expression of novel inhibitory pathways specifically on stem-like cells, contributing to the maintenance of their stemness and quiescence during chronic LCMV infection (44). Interestingly, the expression of these novel inhibitory receptors on stem-like CD8 T cells was regulated by TGF-β signaling and was time-dependent becoming more prominent at later time points during chronic LCMV infection (44). These studies point to the importance of the temporal aspects when characterizing CD8 T cells under conditions of chronic antigen exposure during chronic infection and cancer.

Although heterogeneity of CD8 T cells including the subsets of stem-like and terminally differentiated cells have been identified in different types of human tumors (16–22), their spatial distribution within the TME has not been fully evaluated. We recently found that $TCF1^+$ $PD\text{-}1^+$ CD8 TILs were predominantly localized in the stromal areas and were rarely present in the tumor parenchyma in both primary tumors and metastatic lymph nodes of HNSCC patients (18). We now show in this study of lung cancer patients that $PD\text{-}1^+TCF1^+$ CD8 T cells were mainly found in the TLSs within the tumor. Similar to other investigators' observations that TLSs are present in 67 to 90% of NSCLC tumor samples (45, 46), we identified TLSs in 69% of our tumor samples. We found that $PD\text{-}1^+TCF1^+$ stem-like CD8 T cells clustered near CD4 T cells, while the $PD\text{-}1^+TCF1^-$ more differentiated cells were diffusely scattered in the tumor parenchyma of human lung tumors. The observation of stem-like $CD8^+$ cells in close proximity to $CD4^+$ cells in the TLSs may simply be because the stem-like CD8 T cells mainly

reside in the T cell-like zones of the TLSs. However, it could also suggest direct interactions between stem-like CD8 T cells and antigen-specific CD4 T cells. In the chronic LCMV mouse model, we have shown that stem-like CD8 T cells are located primarily in lymphoid tissues, specifically the white pulp of the spleen where infected cells are rarely present, whereas terminally differentiated CD8 T cells were mainly present in the red pulp of the spleen at the site of viral infection (*SI Appendix*, Fig. S3) (10). These data strongly suggest that stem-like CD8 T cells in both tumors and chronic viral infection preferentially reside in the area in specific niches surrounded by lymphoid and myeloid cells where direct interaction between TCF1$^+$ stem-like CD8 T cells and virally infected cells or tumors is limited. In contrast, terminally differentiated CD8 T cells are more dispersed throughout the tumor parenchyma and stromal areas where they can more readily engage with target cells. Our finding suggest that TLSs provide a supportive niche for TCF1$^+$ stem-like cells for controlled antigen encounter. Consistent with this, Asrir et al. presented that maturation and increased proportion of endothelial cells that form tumor-associated high endothelial venules support infiltration of TCF1$^+$ stem-like cells into the tumor microenvironment (47). To further highlight the importance of TLSs for tumor control, recent reports have shown a positive association between TLSs and clinical response and survival (48–50). In addition, B cell-rich samples contained more TCF1-expressing CD8 T cells compared to B cell-poor samples (48). More importantly, many of these studies have shown that clinical reponse to immunotherapy is associated with more TCF1$^+$ stem-like CD8 T cells (19–22, 47) and TLSs (48–50). Taken together, considering the exclusive proliferation of stem-like CD8 T cells upon PD-1 blockade in chronic viral infection and tumor, it is plausible that the abundance of TLS could be a marker for predicting immune checkpoint blockade because they preferentially possess the stem-like CD8 T cells.

In addition to avoiding the antigenic exposure, TLSs might provide a niche for the maintenance of stem-like CD8 TILs. In kidney, bladder, and prostate cancer patients, TCF1$^+$PD-1$^+$ CD8 TILs were found in close proximity to MHC-II-expressing cells, which might be antigen-presenting cell niches (51). We made an interesting observation that further supports the interactions between DCs and stem-like CD8 T cells in lymphoid-like compartments such as TLSs. In our preclinical and clinical samples in addition to HNSCC patients (18), we observed high *Xcl1* expression in the stem-like subset compared to the terminally exhausted subset. XCR1 is the sole known receptor of XCL1 and is selectively expressed on the surface of CD8α$^+$ lymphoid DCs, also referred to as type 1 conventional dendritic cells (cDC1) (52). Recently, in the model of chronic LCMV infection, Dahling et al. presented that cDC1 play a pivotal role for sustaining stem-like CD8 T cells through MHC-I-dependent interaction (53). In tumor models, several reports have also demonstrated the essential role of CD103$^+$ DCs, which are considered in the same lineage with CD8α$^+$ lymphoid DCs, for the induction of antitumor activity and responsiveness to PD-1 pathway blockade (54–56). In human cancer patients with breast cancer, HNSCC, or lung adenocarcinoma, the abundance of transcripts related to CD103$^+$ DCs has been associated with favorable clinical outcomes (56). Based on these results, we propose that XCR1$^+$ lymphoid DCs play a significant role in sustaining stem-like CD8 T cells and inducing the proliferative burst upon PD-1/PD-L1 inhibition. Consistently, cDC1s in tumor-draining lymph nodes play a role in maintaining TCF1$^+$ CD8 T cell subset in an autochthonous model of lung adenocarcinoma (57).

In conclusion, we found that TCF1$^+$ CD8 T cells share similar phenotype, transcriptional profiles, and biological functions in cancer and chronic viral infection. Importantly, the TCF1$^+$PD-1$^+$ stem-like CD8 T cells are primarily present in TLSs in human lung cancer samples highlighting the importance of TLSs in providing a niche for the maintenance of this stem-like CD8 T cell population and more broadly for cancer immunotherapy.

Materials and Methods

A detailed description of materials and methods is provided in *SI Appendix, Materials and Methods*. Mouse skin melanoma B16F10-GP (5×10^5), lung carcinoma LLC1-GP (5×10^5), prostate adenocarcinoma TRAMP-C2 (5×10^5), and colon carcinoma CT26 (5×10^5) cells were used. For chronic LCMV infection, mice were infected with 2×10^6 pfu LCMV Cl-13 intravenously after transient CD4 T cell depletion. All animal experiments were performed in accordance with Emory University Institutional Animal Care and Use Committee.

Primary and metastatic tumors in lung tissues were obtained from 19 patients with stage I–IV disease who underwent surgical resection as standard care. None of the patients received checkpoint inhibitors prior to surgery. Patients were consented for tissue and blood collection under an Emory University Winship Cancer Institute tissue collection protocol, in accordance with the Emory University Institutional Review Board.

Data, Materials, and Software Availability. Transcriptional data have been deposited in Gene Expression Omnibus (GEO) database (GSE227399 and GSE228419) (58, 59).

ACKNOWLEDGMENTS. Research reported in this publication was supported in part by the National Cancer Institute (NCI) of the NIH under Award Number P50CA217691 and the Integrated Cellular Imaging Microscopy Core (2P30CA138282-04), the Cancer Tissue and Pathology shared resource (P30CA13829) of the Winship Cancer Institute of Emory University and NIH/NCI, and the Monell Foundation. The content is solely the responsibility of the authors and does not necessarily represent the official views of the NIH. This work was also supported by the National Research Foundation of Korea grant funded by the Korean government (The Ministry of Science and ICT) (RS-2023-00211426) and the National Cancer Center grant (NCC-19112605).

Author affiliations: [a]Emory Vaccine Center, Emory University School of Medicine, Atlanta, GA 30322; [b]Department of Microbiology and Immunology, Emory University School of Medicine, Atlanta, GA 30322; [c]Department of Immunology, Sungkyunkwan University School of Medicine, Suwon 16419, Republic of Korea; [d]Department of Pathology and Laboratory Medicine, Emory University School of Medicine, Atlanta, GA 30322; [e]Department of Pathology, Case Western Reserve University School of Medicine, Cleveland, OH 44106; [f]Department of Immunology and Immunotherapy, Lipschultz Precision Immunology Institute, Tisch Cancer Institute, Icahn School of Medicine at Mount Sinai, New York, NY 10029; [g]Department of Oncological Sciences, Lipschultz Precision Immunology Institute, Tisch Cancer Institute, Icahn School of Medicine at Mount Sinai, New York, NY 10029; [h]Department of Urology, Emory University School of Medicine, Atlanta, GA 30322; [i]Department of Hematology and Medical Oncology, Emory University School of Medicine, Atlanta, GA 30322; [j]Winship Cancer Institute, Emory University School of Medicine, Atlanta, GA 30322; [k]Department of Pathology, University of Pittsburgh School of Medicine, Pittsburgh, PA 15213; and [l]Hospital Israelita Albert Eisnstein, Sao Paulo 05652, Brazil

1. M. Hashimoto *et al.*, CD8 T cell exhaustion in chronic infection and cancer: Opportunities for interventions. *Annu. Rev. Med.* **69**, 301–318 (2018).
2. L. M. McLane, M. S. Abdel-Hakeem, E. J. Wherry, CD8 T cell exhaustion during chronic viral infection and cancer. *Annu. Rev. Immunol.* **37**, 457–495 (2019), 10.1146/annurev-immunol-041015-055318.
3. A. J. Zajac *et al.*, Viral immune evasion due to persistence of activated T cells without effector function. *J. Exp. Med.* **188**, 2205–2213 (1998).
4. A. Gallimore *et al.*, Induction and exhaustion of lymphocytic choriomeningitis virus-specific cytotoxic T lymphocytes visualized using soluble tetrameric major histocompatibility complex class I-peptide complexes. *J. Exp. Med.* **187**, 1383–1393 (1998).
5. D. L. Barber *et al.*, Restoring function in exhausted CD8 T cells during chronic viral infection. *Nature* **439**, 682–687 (2006).
6. J. R. Brahmer *et al.*, Safety and activity of anti-PD-L1 antibody in patients with advanced cancer. *N Engl. J. Med.* **366**, 2455–2465 (2012).
7. S. L. Topalian *et al.*, Safety, activity, and immune correlates of anti-PD-1 antibody in cancer. *N Engl. J. Med.* **366**, 2443–2454 (2012).
8. N. Prokhnevska *et al.*, CD8(+) T cell activation in cancer comprises an initial activation phase in lymph nodes followed by effector differentiation within the tumor. *Immunity* **56**, 107–124.e105 (2023).

9. K. A. Connolly *et al.*, A reservoir of stem-like CD8(+) T cells in the tumor-draining lymph node preserves the ongoing antitumor immune response. *Sci. Immunol.* **6**, eabg7836 (2021).
10. S. J. Im *et al.*, Defining CD8+ T cells that provide the proliferative burst after PD-1 therapy. *Nature* **537**, 417–421 (2016).
11. R. He *et al.*, Follicular CXCR5- expressing CD8(+) T cells curtail chronic viral infection. *Nature* **537**, 412–428 (2016).
12. D. T. Utzschneider *et al.*, T cell factor 1-expressing memory-like CD8(+) T cells sustain the immune response to chronic viral infections. *Immunity* **45**, 415–427 (2016).
13. W. H. Hudson *et al.*, Proliferating transitory T cells with an effector-like transcriptional signature emerge from PD-1(+) stem-like CD8(+) T cells during chronic infection. *Immunity* **51**, 1043–1058.e1044 (2019).
14. S. J. Im, S. J. Ha, Re-defining T-cell exhaustion: Subset, function, and regulation. *Immune Netw.* **20**, e2 (2020).
15. M. Hashimoto *et al.*, PD-1 combination therapy with IL-2 modifies CD8(+) T cell exhaustion program. *Nature* **610**, 173–181 (2022).
16. C. S. Jansen *et al.*, An intra-tumoral niche maintains and differentiates stem-like CD8 T cells. *Nature* **576**, 465–470 (2019).
17. I. Siddiqui *et al.*, Intratumoral Tcf1(+)PD-1(+)CD8(+) T cells with stem-like properties promote tumor control in response to vaccination and checkpoint blockade immunotherapy. *Immunity* **50**, 195–211.e110 (2019).
18. C. S. Eberhardt *et al.*, Functional HPV-specific PD-1(+) stem-like CD8 T cells in head and neck cancer. *Nature* **597**, 279–284 (2021).
19. B. C. Miller *et al.*, Subsets of exhausted CD8(+) T cells differentially mediate tumor control and respond to checkpoint blockade. *Nat. Immunol.* **20**, 326–336 (2019).
20. M. Sade-Feldman *et al.*, Defining T cell states associated with response to checkpoint immunotherapy in melanoma. *Cell* **175**, 998–1013.e1020 (2018).
21. X. Fang *et al.*, TCF-1(+) PD-1(+) CD8(+)T cells are associated with the response to PD-1 blockade in non-small cell lung cancer patients. *J. Cancer Res. Clin. Oncol.* **148**, 2653–2660 (2022).
22. J. Koh *et al.*, TCF1(+)PD-1(+) tumour-infiltrating lymphocytes predict a favorable response and prolonged survival after immune checkpoint inhibitor therapy for non-small-cell lung cancer. *Eur. J. Cancer* **174**, 10–20 (2022).
23. S. Gautam *et al.*, The transcription factor c-Myb regulates CD8(+) T cell stemness and antitumor immunity. *Nat. Immunol.* **20**, 337–349 (2019).
24. Y. Liu *et al.*, LSD1 inhibition sustains T cell invigoration with a durable response to PD-1 blockade. *Nat. Commun.* **12**, 6831 (2021).
25. P. Falvo *et al.*, Cyclophosphamide and vinorelbine activate stem-like CD8(+) T cells and improve anti-PD-1 efficacy in triple-negative breast cancer. *Cancer Res.* **81**, 685–697 (2021).
26. Q. Shan *et al.*, Ectopic Tcf1 expression instills a stem-like program in exhausted CD8(+) T cells to enhance viral and tumor immunity. *Cell Mol. Immunol.* **18**, 1262–1277 (2021).
27. Q. Feng *et al.*, Lactate increases stemness of CD8 + T cells to augment anti-tumor immunity. *Nat. Commun.* **13**, 4981 (2022).
28. J. W. Griffith, C. L. Sokol, A. D. Luster, Chemokines and chemokine receptors: Positioning cells for host defense and immunity. *Annu. Rev. Immunol.* **32**, 659–702 (2014).
29. F. Alfei *et al.*, TOX reinforces the phenotype and longevity of exhausted T cells in chronic viral infection. *Nature* **571**, 265–269 (2019).
30. O. Khan *et al.*, TOX transcriptionally and epigenetically programs CD8(+) T cell exhaustion. *Nature* **571**, 211–218 (2019).
31. A. C. Scott *et al.*, TOX is a critical regulator of tumour-specific T cell differentiation. *Nature* **571**, 270–274 (2019).
32. J. R. Teijaro *et al.*, Persistent LCMV infection is controlled by blockade of type I interferon signaling. *Science* **340**, 207–211 (2013).
33. E. B. Wilson *et al.*, Blockade of chronic type I interferon signaling to control persistent LCMV infection. *Science* **340**, 202–207 (2013).
34. A. O. Kamphorst *et al.*, Rescue of exhausted CD8 T cells by PD-1-targeted therapies is CD28-dependent. *Science* **355**, 1423–1427 (2017).
35. E. Hui *et al.*, T cell costimulatory receptor CD28 is a primary target for PD-1–mediated inhibition. *Science* **355**, 1428–1433 (2017).
36. S. J. Im, B. T. Konieczny, W. H. Hudson, D. Masopust, R. Ahmed, PD-1+ stemlike CD8 T cells are resident in lymphoid tissues during persistent LCMV infection. *Proc. Natl. Acad. Sci. U.S.A.* **117**, 4292–4299 (2020).
37. O. Meyuhas, T. Kahan, The race to decipher the top secrets of TOP mRNAs. *Biochim. Biophys. Acta* **1849**, 801–811 (2015).
38. R. Miloslavski *et al.*, Oxygen sufficiency controls TOP mRNA translation via the TSC-Rheb-mTOR pathway in a 4E-BP-independent manner. *J. Mol. Cell Biol.* **6**, 255–266 (2014).
39. C. C. Thoreen *et al.*, A unifying model for mTORC1-mediated regulation of mRNA translation. *Nature* **485**, 109–113 (2012).
40. M. M. Staron *et al.*, The transcription factor FoxO1 sustains expression of the inhibitory receptor PD-1 and survival of antiviral CD8(+) T cells during chronic infection. *Immunity* **41**, 802–814 (2014).
41. S. Ando *et al.*, mTOR regulates T cell exhaustion and PD-1 targeted immunotherapy response during chronic viral infection. *J. Clin. Invest.* **133**, e160025 (2022), 10.1172/JCI160025.
42. J. Dickow *et al.*, Diverse immunomodulatory effects of individual IFNalpha subtypes on virus-specific CD8(+) T cell responses. *Front. Immunol.* **10**, 2255 (2019).
43. Z. Huang *et al.*, IL-27 promotes the expansion of self-renewing CD8(+) T cells in persistent viral infection. *J. Exp. Med.* **216**, 1791–1808 (2019).
44. Y. Hu *et al.*, TGF-beta regulates the stem-like state of PD-1+ TCF-1+ virus-specific CD8 T cells during chronic infection. *J. Exp. Med.* **219**, e20211574 (2022).
45. X. Sun *et al.*, Maturation and abundance of tertiary lymphoid structures are associated with the efficacy of neoadjuvant chemoimmunotherapy in resectable non-small cell lung cancer. *J. Immunother. Cancer* **10**, e005531 (2022).
46. F. Ren *et al.*, Tertiary lymphoid structures in lung adenocarcinoma: Characteristics and related factors. *Cancer Med.* **11**, 2969–2977 (2022).
47. A. Asrir *et al.*, Tumor-associated high endothelial venules mediate lymphocyte entry into tumors and predict response to PD-1 plus CTLA-4 combination immunotherapy. *Cancer Cell* **40**, 318–334.e319 (2022).
48. R. Cabrita *et al.*, Tertiary lymphoid structures improve immunotherapy and survival in melanoma. *Nature* **577**, 561–565 (2020).
49. B. A. Helmink *et al.*, B cells and tertiary lymphoid structures promote immunotherapy response. *Nature* **577**, 549–555 (2020).
50. F. Petitprez *et al.*, B cells are associated with survival and immunotherapy response in sarcoma. *Nature* **577**, 556–560 (2020).
51. C. Calagua *et al.*, A subset of localized prostate cancer displays an immunogenic phenotype associated with losses of key tumor suppressor genes. *Clin. Cancer Res.* **27**, 4836–4847 (2021).
52. L. Chen, D. B. Flies, Molecular mechanisms of T cell co-stimulation and co-inhibition. *Nat. Rev. Immunol.* **13**, 227–242 (2013).
53. S. Dahling *et al.*, Type 1 conventional dendritic cells maintain and guide the differentiation of precursors of exhausted T cells in distinct cellular niches. *Immunity* **55**, 656–670.e658 (2022).
54. M. L. Broz *et al.*, Dissecting the tumor myeloid compartment reveals rare activating antigen-presenting cells critical for T cell immunity. *Cancer Cell* **26**, 638–652 (2014).
55. E. W. Roberts *et al.*, Critical role for CD103(+)/CD141(+) dendritic cells bearing CCR7 for tumor antigen trafficking and priming of T cell immunity in melanoma. *Cancer Cell* **30**, 324–336 (2016).
56. H. Salmon *et al.*, Expansion and activation of CD103(+) dendritic cell progenitors at the tumor site enhances tumor responses to therapeutic PD-L1 and BRAF inhibition. *Immunity* **44**, 924–938 (2016).
57. J. M. Schenkel *et al.*, Conventional type I dendritic cells maintain a reservoir of proliferative tumor-antigen specific TCF-1(+) CD8(+) T cells in tumor-draining lymph nodes. *Immunity* **54**, 2338–2353.e2336 (2021).
58. S. J. Im, R. Ahmed, Defining CD8+ T cells that provide the proliferative burst after PD-1 therapy. Gene Expression Omnibus (GEO). https://www.ncbi.nlm.nih.gov/geo/query/acc.cgi?acc=GSE227399. Deposited 15 March 2023.
59. S. J. Im, R. Ahmed, Characteristics and anatomic location of PD-1+TCF1+ stem-like CD8 T cells in chronic viral infection and cancer. Gene Expression Omnibus (GEO). https://www.ncbi.nlm.nih.gov/geo/query/acc.cgi?acc=GSE228419. Deposited 28 March 2023.